


# Friction influence on brake squeal in disc and drum brakes using complex eigenvalue analysis

Romulo do Nascimento Rodrigues<sup>\*1,2</sup>, Anderson Luiz Dias<sup>3</sup>, Camilo Augusto Santos Costa<sup>4</sup>,  
Roberto de Araujo Bezerra<sup>2</sup>

<sup>1</sup>Czech Technical University in Prague, Faculty of Mechanical Engineering, Centre of Vehicles for Sustainable Mobility, Prague, Czech Republic.

<sup>2</sup>Universidade Federal do Ceará, Departamento de Engenharia Mecânica, Laboratório de Vibrações, Fortaleza, CE, Brasil.

<sup>3</sup>University of Modena and Reggio Emilia, Department of Engineering Enzo Ferrari, Modena, Italy.

<sup>4</sup>Universidade Federal do Ceará, Laboratório Térmico e de Fluidos, Fortaleza, CE, Brasil.

Received on January 24, 2025. Accepted on March 06, 2025.

Brake noise, is a complex issue in automotive and industrial systems caused by friction-induced vibrations between the brake pad and disc. This noise impacts vehicle performance, accelerates component wear, and diminishes consumer satisfaction. Squeal can be categorized into low frequency (1–5 kHz) and high frequency (6–20 kHz) types, explained by mechanisms such as stick-slip, sprag-slip, and mode coupling, which involve interactions among friction, component geometry, and vibration modes. While experimental studies often face budget constraints, advancements in computational techniques like the Finite Element Method (FEM) provide new insights into brake noise dynamics. FEM, combined with complex eigenvalue analysis, offers a cost-effective way to study brake squeal. This study aims to develop a FEM model to analyze brake squeal, focusing on variations in friction coefficients in solid and ventilated disc brakes for cars, motorcycles, and trains, as well as drum brake systems. The findings indicate that solid motorcycle disc brakes exhibit minimal low squeal, with high squeal occurring only at maximum friction levels, while vented motorcycle disc brakes show high squeal at all levels, maintaining lower Total Unstable Frequencies (TUF) and Noise Index (NI). The model offers valuable insights that can be applied in both education and research.

**Keywords:** Brake squeal, Friction-induced vibrations, Finite Element Method, Complex eigenvalue analysis, Brake systems.

## 1. Introduction


Brake noise is a complex phenomenon that occurs during the braking process in automotive and industrial systems. It primarily manifests as unwanted acoustic vibrations, which can range from high-pitched sounds (squeal) to low-frequency noises (groans). These noises not only affect consumer's perception of vehicle quality but also indicate potential performance issues and excessive component wear. The study of brake noise is fundamental in automotive engineering, as it involves the interaction of multiple factors, including friction materials, the structural characteristics of the disc and brake pads, contact forces, the stiffness and damping properties of the components, and the contact dynamics between surfaces.

Interfacial friction events are known to be quite complex, and brake squealing can be triggered when a rotating brake disc rubs against the brake pad under certain operating conditions. Due to the friction generated between the pads and the disc, the kinetic energy

of the vehicle is primarily dissipated as heat, causing the vehicle to lose speed [1]. The difference between static and dynamic friction coefficients is well established in scientific knowledge, with the first two laws proposed by Amonton in 1699 [2]. According to Akay [1], when the friction condition provides more energy than the system is able to dissipate in the form of thermal energy, part of this energy is converted into dynamic instability (vibrations) which in turn generate sound radiation. The discontinuity in the friction regime is closely related to the occurrence of vibrations in brake systems, as it causes energy dissipation peaks. However, as living standards improve and environmentally friendly regulations are established, consumers are increasingly prioritizing noise pollution reduction and comfort levels in vehicle.

Engineers and researchers have classified brake noise into several categories, with squeal being the most significant due to its friction-induced nature [1, 3–6]. Squeal is an auto-excited noise that creates self-sustained vibrations for a short period [7–9]. Two definitions of squeal exist: Low-frequency squeal, with spectrum bands varying from 1 to 5 kHz, and high-frequency squeal, occurring between 6 and 20 kHz [1, 6, 10, 11]. Currently,

\*Correspondence email address: [rrodrigues@ufc.br](mailto:rrodrigues@ufc.br)

Editor-in-Chief: Marcello Ferreira

there are three explanations for the occurrence of brake squeal: Stick-slip, sprag-slip, and mode coupling [1, 6, 11]. The stick-slip explanation is primarily based on the assumption that the coefficient of friction between the brake pad and the brake disc decreases with increasing sliding speed. In systems where the coefficient of friction declines with increased speed, negative damping factors can occur, leading to unstable oscillation modes and resulting in brake squeal [12–14]. The sprag-slip explanation arises from the geometrical deformation of the brake components, primarily the friction material. This deformation leads to variations in normal and tangential forces, making the system prone to brake squeal [15]. The third explanation, mode coupling, occurs when the vibration modes of the brake components coincide. It has been shown that this can happen even if the friction coefficient remains constant [16]. It has also been demonstrated that a brake squeal occurs only when at least two of these events occur simultaneously [1, 12].

Experimental investigations into the dynamic instability of brake systems influenced by various parameters frequently encounter substantial difficulties, with budget limitations being a primary obstacle. In recent years, due to great advances in computing, researchers have used the Finite Element Method to deal with the phenomenon of vibration generation [17–22]. Liles [23] was one of the first to use the finite element method to try to understand the phenomenon of vibrational instabilities in brake systems. According to Liles [23], knowing the unstable modes of the brake system facilitates several courses of action during design; the modal frequencies could be moved by changing the components or damping could be added so that the unstable mode in question becomes stable.

According to Ouyang [12], the simulations and analysis methods for the Squeal of the brakes can be divided into two broad categories: Analysis of complex eigenvalues in the frequency domain and transient analysis in the time domain. In the complex eigenvalue analysis, it is possible to find some or all of the eigenvalues at once, while the transient analysis program must be run several times, until a cycle limit movement is found. Therefore, the complex eigenvalue method yields lower computational costs [12]. Over the past thirty years, numerous numerical studies have been conducted across a wide range of brake systems, aiming to better understand the underlying phenomena and the factors that influence them [4, 5, 14, 17–22, 24–29].

The aim of this work is to develop a finite element model that facilitates the analysis of the brake squeal phenomenon through complex eigenvalue analysis in the frequency domain. The main focus will be to investigate the influence of friction coefficient variation in different brake systems, including solid and ventilated disc brakes for cars, motorcycles, and trains, as well as heavy, simplex, and duplex drum brakes. By relating these friction variations to the occurrence of brake squeal, the model is expected to provide a more detailed understanding of the factors that contribute to the

unstable behavior of these systems. This study aims to make a valuable contribution, allowing the model to be applied in both educational contexts and academic and industrial research.

## 2. Nomenclature

The main notations adopted in this document are reported in in Table 1.

**Table 1:** Parameter nomenclature.

Symbol	Name
Pressure	P
Contact pressure	p
Static pressure at interface	p <sub>0</sub>
Maximum pressure	p <sub>max</sub>
Normal contact force	F <sub>n</sub>
Frictional contact force	F <sub>f</sub>
Normal stress	$\sigma_x$
Shear stress	$\tau_{xy}$
Elongation or compression offset of the component	dL
Length of the component	L
Friction coefficient	$\mu$
Disc Speed	$\omega$
Force	F
Disc Young's modulus	E <sub>Disc</sub>
Back Plate Young's modulus	E <sub>Back Plate</sub>
Pad Material Young's modulus	E <sub>Pad</sub>
Disc density	$\gamma_{Disc}$
Back Plate density	$\gamma_{Back Plate}$
Pad Material density	$\gamma_{Pad}$
Disc Poisson's ratio	$\nu_{Disc}$
Back Plate Poisson's ratio	$\nu_{Back Plate}$
Pad Material Poisson's ratio	$\nu_{Pad}$
Disc thickness	h <sub>Disc</sub>
Back Plate thickness	h <sub>Back Plate</sub>
Pad Material thickness	h <sub>Pad</sub>
Disc diameter	D <sub>Disc</sub>
Pad Material contact area	A <sub>pad</sub>
Complex eigenvalues	$\lambda_i$
Real part eigenvalue	$\sigma_i$
Imaginary part eigenvalue	$\omega_i$
Nodal normal force row matrix	{f <sub>n</sub> }
Nodal friction force row matrix	{f <sub>f</sub> }
System mass square matrix	[M]
System rigidity square matrix	[K]
System damping square matrix	[C]
System friction matrix	[K <sub>f</sub> ]
System contact stiffness matrix	[K <sub>c</sub> ]
System contact-friction matrix	[K <sub>fc</sub> ]
Eigenvector rectangular matrix	[V] <sup>T</sup>
System nodal acceleration row matrix	{ $\ddot{U}$ }
System nodal velocity row matrix	{ $\dot{U}$ }
System nodal displacement row matrix	{U}
System applied resulting force row matrix	{F}
Nodal braking force	{F <sub>brake</sub> }
Displacement boundary conditions	B.C.

### 3. Methodology

The process driven by this analysis (Figure 1) begins with the development of brakes finite element model. For the analysis, solid and ventilated disc brakes for cars, motorcycles, and trains were considered, as well as heavy, simplex, and duplex drum brakes (see Figure 2). Five components are considered in the brake disc assembly: the disc itself, two backing plates, and two brake pads. For the drum brakes, five components are also considered: the drum itself, two friction linings, and two brake shoes. It is worth mentioning that the models developed for this work are intentionally in a basic level. This is quite important not only to avoid additional complexities due to detailed constraints, but also to facilitate the introduction of variable geometries.

Figure 3 presents the boundary conditions considered in this work. The same understanding will be applied to all other disc brake systems, as well as to the drum brakes. It is important to note that for the drum brakes, the analysis will consider variations only at the pressure application point, given that their operational mechanisms differ from those of disc brakes. This model include, as input parameters, the material modulus of elasticity ( $E$ ) and friction coefficient ( $\mu$ ) owing to contact between the brake pad and the disc during its rotation.

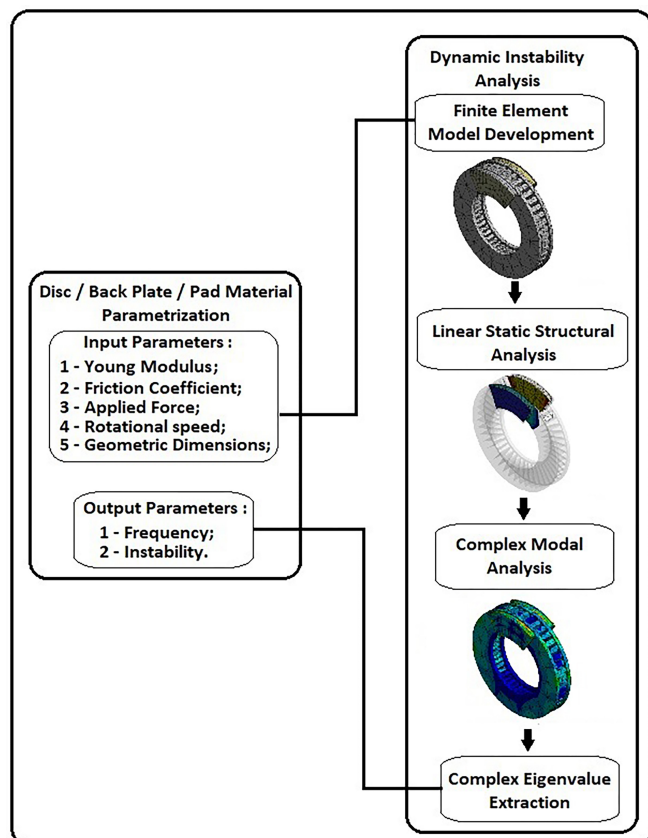


**Figure 1:** Flowchart for the Analysis of Drum and Disc Brake Systems.

The brake disc is fixed to the hub that is modeled with a fixed support (Sticker A on Figure 3). The brake pad (Friction Material and Back Plate) are modeled with the remote displacement (Sticker B on Figure 3), though with activation force on the opposite extremity (Sticker A on Figure 3). The term remote displacement is an approach adopted when the component to be displaced is activated indirectly. In our case, both brake pads and linings are touch the disc and drus, respectively, through a force applied on their fixtures. The support fixes the body for translational and rotational movements while providing freedom for displacement normal to the disc.

The brake disc mesh comprises 5,439 elements and 13,310 nodes for the ventilated disc. The elements of contact between the friction material and disc are CONTA174 and TARGE170, respectively. According to Ansys APDL Theory Reference CONTA174 is a 3-D and 8-node element located on the surfaces of solids. It is adopted quadrilateral elements on friction material surfaces through the command KEYOPT (4). For the disc internal surface, TARGE170 permits the rotational displacement input ( $\omega$ ) on the elements using CMROTATE command. Furthermore, it is performed by the following processes, (1) a static analysis of the brake disc operation, without disc rotation, to achieve the pre-stress conditions, and (2) a frequency calculation of the complex eigenvalues during disc rotation while the brake pad are coupled on it. Moreover, with all calculations finished, the output parameters are extracted. The quadrilateral elements are flexible for mesh generation and also fitted our actual processing capability. Improvements in the model mesh are tasks of our future updates. These are consisted by unstable vibration modes, that is, the complex eigenvalues with a positive real part and its frequencies. Hence, these data are used for the generation of the bar chart, relating input and output parameters, dot plot chart, and relating the imaginary part and real part of the eigenvalue and the response surface graphs that are statistical representations of the output parameter behaviors in relation to input parameters.

The brake disc design procedure is applied on models illustrated by Figure 3. The small circle illustrates the contact between the pad material and the disc being  $F_n$  the normal force,  $F_f$  is the friction force and  $K_c$  the contact stiffness. Hence, considering that disc is rotating with constant velocity, unidirectional sliding, and permanent contact, then according to Coulomb's law of friction:

$$f_t = -\mu f_n \quad (1)$$

There are two stresses generated in section of contact, therefore, Coulomb's law can also be written in terms of shear stress  $\tau$  and normal stress  $\sigma$  as follows:

$$\tau = -\mu p \quad (2)$$

$$\sigma = p \quad (3)$$

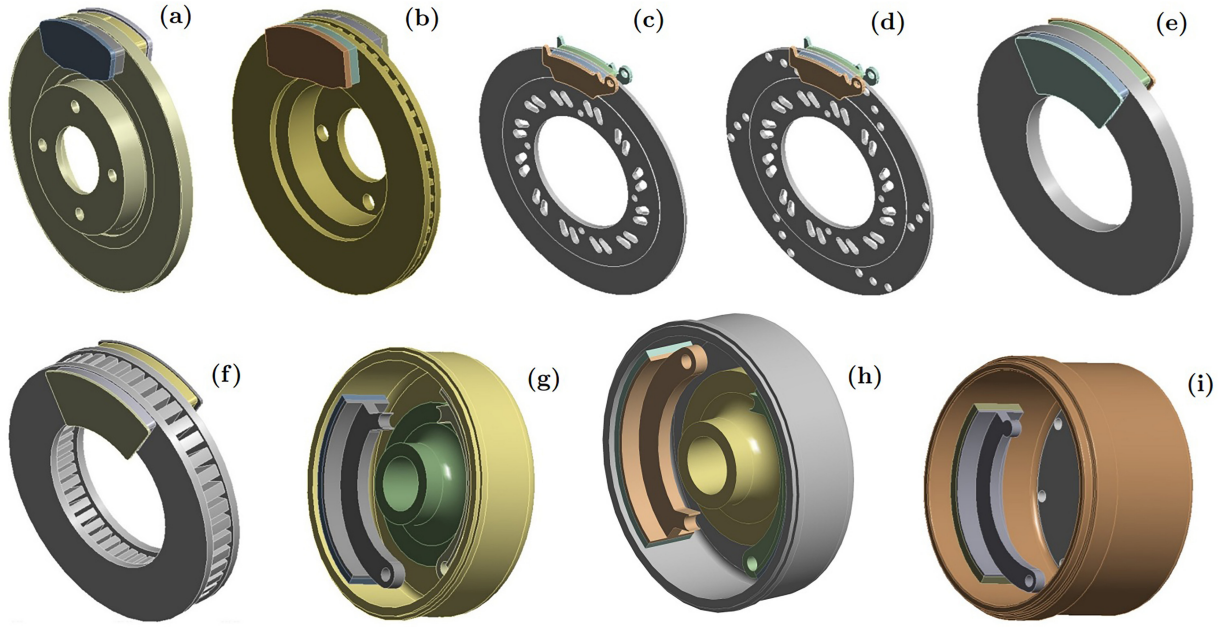


**Figure 2:** Simulated Disc and Drum Brake Models; (a) Solid car disc brake; (b) Vented car disc brake; (c) Solid motorcycle disc brake; (d) Vented motorcycle disc brake; (e) Solid railway disc brake; (f) Vented railway disc brake; (g) Simplex drum brake; (h) Duplex drum brake; (i) Heavy drum brake.

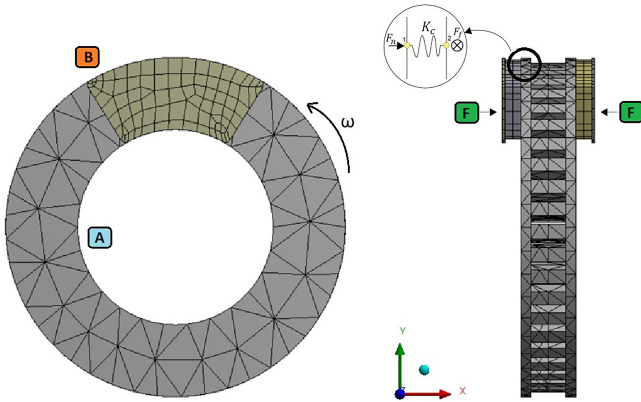


**Figure 3:** Boundary conditions of the vented railway brake disc.

The equivalent stress is evaluated by ANSYS using von Mises theory:

$$\sigma' = \sqrt{\sigma_x^2 + 3\tau_{xy}^2} \quad (4)$$

Finally, it is known that Young's modulus  $E$  is a relation between stress ( $\sigma$ ) and strain ( $\epsilon$ ); thus, pad material Young's modulus can be expressed by:

$$E_{\text{pad}} = \frac{\sigma'}{\epsilon} = \frac{\sqrt{\sigma_x^2 + 3\tau_{xy}^2}}{dL/L_0} \quad (5)$$

To model the contact between the pad material and disc, an interface of finite elements of mass, mechanical springs, and dash-pots is used. The rigidity of the contact

$k_c$  is estimated by:

$$k_c = \frac{E_{\text{pad}} A_{\text{pad}}}{h_{\text{pad}}} \quad (6)$$

Hence, substituting the  $E_{\text{pad}}$  (equation 5) in equation 6, it can be observed that  $p$  impacts on contact rigidity:

$$k_c = \frac{p L_0 A_{\text{pad}} \sqrt{1 + 3\mu^2}}{d L h_{\text{pad}}} \quad (7)$$

The pad material is discretized into a set of spring-modified elements of rigidity  $k_c$  and friction coefficient  $\mu$  [3]. The equation below:

$$f_n = k_c u_n \rightarrow f_t = -\mu f_n = -\mu k_c u_n \quad (8)$$

results in elementary matrix equations 9 and 10. Equation 9 is given as

$$\begin{bmatrix} 1 & -1 \\ -1 & 1 \end{bmatrix} \begin{bmatrix} U_{2n} \\ U_{1n} \end{bmatrix} = \begin{bmatrix} F_{2n} \\ F_{1n} \end{bmatrix} \quad (9)$$

Expanding to the node canvas and adding  $[K_c]$  and  $[K_f]$  to form the contact-friction element  $[K_{cf}]$  results in

$$\begin{bmatrix} k_c & 0 & -k_c & 0 \\ -\mu k_c & 0 & \mu k_c & 0 \\ -k_c & 0 & k_c & 0 \\ \mu k_c & 0 & -\mu k_c & 0 \end{bmatrix} \begin{bmatrix} U_{2n} \\ U_{2t} \\ U_{1n} \\ U_{1t} \end{bmatrix} = \begin{bmatrix} F_{2n} \\ F_{2t} \\ F_{1n} \\ F_{1t} \end{bmatrix} \quad (10)$$

After  $K_{fc}$  definition, the approach to model the system without approximation on the pad and to create an FEM model of the pad and join it to the FEM model of the back plate is the Lagrange's multipliers. Therefore, the coupling model between the brake pad and the disc and the contact-friction model are acquired by the full system matrix equation

$$[M]\{\ddot{U}\} + [C]\{\dot{U}\} + ([K] + [K_{fc}])\{U\} = \{F_{brake}\} + B.C. \quad (11)$$

Equation 11 can be solved including  $F_{brake} = F(t)$ , and this type of analysis is reserved for full transient studies. The pseudo-rotating hypothesis that will be adopted consists in considering a fixed mesh for the disc. It is important to mention that the pad material and back plate mesh is also fixed. The rotating part has to be axisymmetric, and the contact nodes stay opposite. In addition, the disc rotation is considered for displacement, velocity, and acceleration of it. This affects the manner that centrifugal forces and gyroscopic damping matrix could be added to the equation 11 [4, 17–19]. From this, a homogeneous equation is obtained removing  $F_{brake}$  from the second member of it. However,  $F_{brake}$  is internally involved at the contact. Hence, before removing it, a static computation is carried out which gives  $p_0$ , the static pressure at the interface, for a given value of the force,  $F_{brake} = F_0$ . The contact and friction stresses now are reformulated:

$$p_n = p_0 + k_c u_n, \tau = -\mu p = -\mu k_c u_n \quad (12)$$

This results in  $[K_{fc}]$  that is modified to  $[K_{fc}] + [K_{p0}]$ , where  $[K_{p0}]$  is the pre-stressed contact-friction stiffness matrix for a given load  $F_0$ . Therefore, the homogeneous equation to be studied is written as follows:

$$[M]\{\ddot{U}\} + [C]\{\dot{U}\} + ([K] + [K_{fc}] + [K_{fc}(F_0)])\{U\} = 0 \quad (13)$$

Those equations require that components of the brake models have node coordinates in agreement with the contact surfaces. This was ensured by the building the brake system inside the Ansys environment, the Design Modeler. Such solution was adopted to avoid model exporting. Additionally, it was adopted due to the possibility to set not only the mesh orientation correctly, but also the brake components being part of the same file. Hence, once this was ensured, the APDL codes set for each component surface configure the contact between the nodes.

### 3.1. Static structural analysis

The static structural analysis is a simulation of these brake systems in which the pad material, fixed on the back plate, initiate a frictional contact with the disc surface without rotation (Figure 3). The inertial and

rigidity influences of components are considered for the eigenvalue and eigenvector calculations [20].

$$([K] + [K_{fc}])\{U\} = \{F_{brake}\} + B.C. \quad (14)$$

Simulation process starts with a static structural analysis, in which the disc is considered immobile and the brake pressure is applied, imposing the contact between the pads and the disc. This situation is represented by the following boundary conditions: The internal face of the fixing hole in the disc were considered as fixed supports (Figure 3), the outer faces of the back plates were constrained in all degrees of freedom, except for translation in the direction normal to the contact surface (Figure 3), and a distributed force is also applied to the surface of the outer faces of the back plates (Figure 3). The brake disc operation (Figure 3) begins with pressure of 0.5 MPa [30] applied on back plate (F sticker); The Ansys contact element terminology is CONTA 174 – TARGET 170, a sophisticated contact based on Lagrange's multipliers.

### 3.2. Complex modal analysis

This analysis uses the static structural stress field and results. The disc rotates at constant 5 rad/s speed [30], while the 0.5 MPa pressure [30] pushes the brake pad against the disc. In this analysis, the movement equation internal dissipation (damping) is neglected without drastic penalties to the results [21]. Hence, the dynamic equation of equilibrium is given by

$$[M]\{\ddot{U}\} + [K_{ns}]\{U\} = \{F\} \quad (15)$$

The contact-friction elements are used to integrate the incompatibility of the meshes and also to take into account the pre-loads and friction that lead to an unsymmetrical matrix. Therefore, the term  $[K_{cf}]$  is renamed to  $[K_{ns}]$  owing to non-symmetry of the contact-stiffness matrix. The asymmetry arises from the pad material and disc contact, with relevant influence of their material characteristics. The eigenvalue problem to be solved is written as follows:

$$[M]\{\ddot{U}\} + [K_{ns}]\{U\} = 0 \quad (16)$$

As  $[K_{ns}]$  is non symmetric contact stiffness, the system will exhibit complex eigenvalues,  $\lambda_i$ , written as

$$\lambda_i = \sigma_i \pm j\omega_i \quad (17)$$

The extraction of the complex eigenvalues and eigenvectors is fulfilled through the Ansys QR damped method that results in a reduced system of equations:

$$[k_{ns}] = [V]^T [K_{ns}] [V] \quad (18)$$

Hence, the complex eigenvectors and eigenvalues of the reduced system are extracted allowing the study of the stability looking for the sign of the real part of the



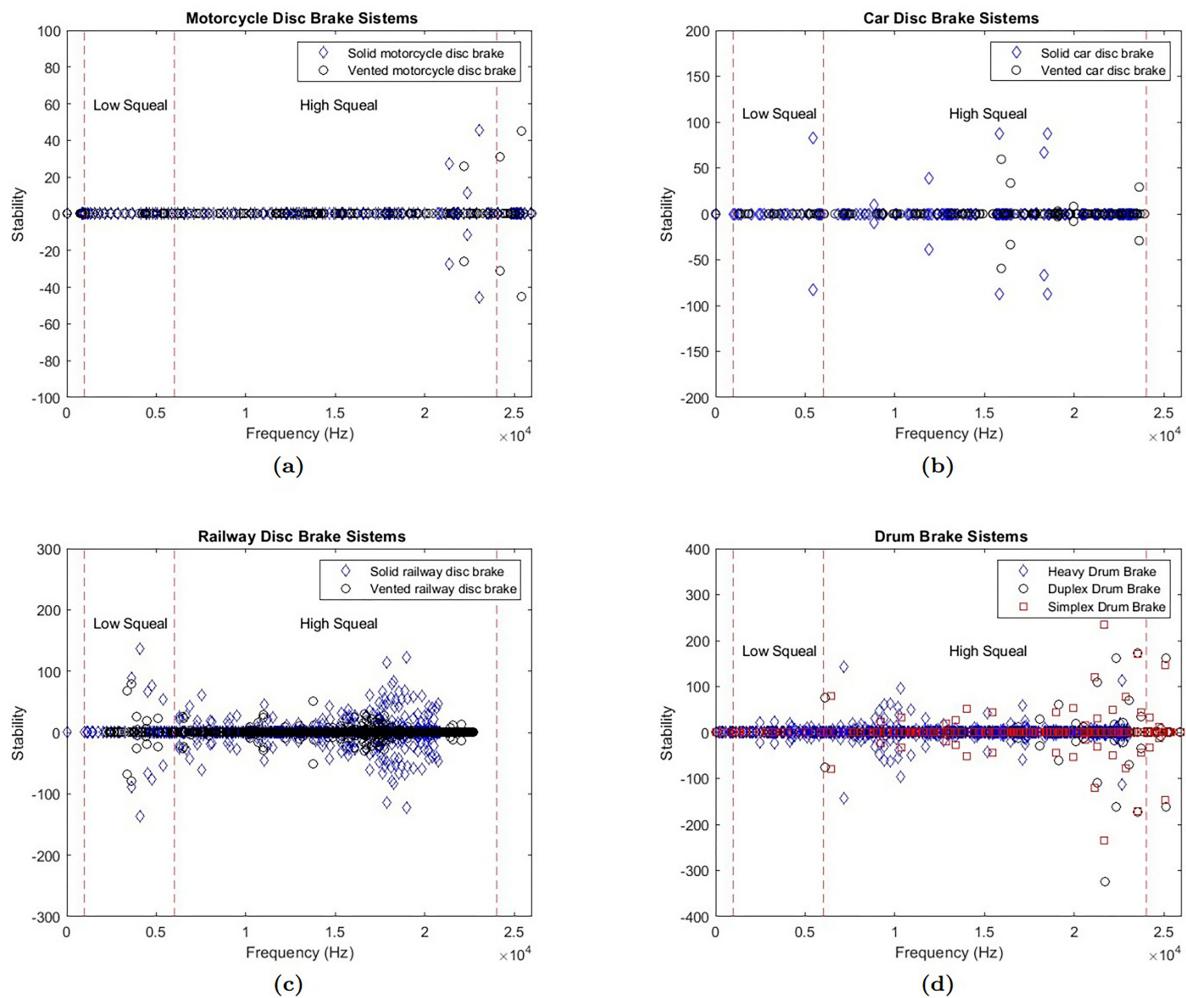


**Figure 4:** Instability occurrence in drum and disc brake systems; (a) Solid and vented motorcycle disc brakes; (b) Solid and vented car disc brakes; (c) Solid and vented railway disc brakes; (d) Heavy, duplex and simplex drum brakes.

eigenvalues (Figure 4). The brake instability occurs when eigenvalues with positive real parts are generated [[23]]. Generally, the real part of the complex eigenvalues is plotted against the associated natural frequencies, in order to visualize the general occurrence of instability. A preliminary implementation of the model, with the reference values from Table 2, was carried out to evaluate the consistency of the model. All operational, geometric, and material parameters of the different brake systems were obtained from the literature [3–6, 17, 18, 25, 30–36].

As can be seen from Figure 4, both brake systems generated several modes of instability. The results of the motorcycle disc brake systems (Table 2) reveal that both solid and vented systems show a low incidence of low squeal, with no occurrences recorded. Regarding high squeal, the solid and vented systems present only 2 and 3 cases, respectively. Furthermore, both types of systems have a TUF of 2 for the solid systems and 3 for the vented systems, indicating similar performance in terms of friction efficiency. The results showed that, for both types of car disc brakes, there was no occurrence of

low-frequency squeal (Table 2). However, high-frequency squeal was observed in both systems, with 4 occurrences in solid brakes and 6 in vented brakes. Additionally, the analysis of Total Unstable Frequencies (TUF) indicated a nearly similar amount of instabilities, with 4 occurrences in solid brakes and 6 in vented brakes. These findings suggest that vented brakes tend to exhibit a slightly higher level of instability and high-frequency squeal, but both systems display similar performance regarding low-frequency squeal.

The results of the railway disc brake systems indicate that both types, solid and vented, exhibit a considerable incidence of high squeal, with 114 cases recorded for the solid systems and 79 for the vented systems. Regarding low squeal, the solid systems have 6 cases, while the vented systems show a slightly better performance, with 8 cases. Additionally, the TUF is 120 for the solid systems and 87 for the vented systems, suggesting that the solid systems have lower friction efficiency compared to the vented systems. The results (Table 2) indicate that heavy drum brake systems exhibit a significant

**Table 2:** Instability occurrence in disc and drum brake systems.

Drum brake systems			
	Heavy	Duplex	Simplex
Low squeal	9	0	0
High squeal	81	18	25
TUF	90	18	25
Car disc brake systems			
	Solid	Vented	
Low squeal	0	0	
High squeal	4	6	
TUF	4	6	
Motorcycle disc brake systems			
	Solid	Vented	
Low squeal	0	0	
High squeal	2	3	
TUF	2	3	
Railway disc brake systems			
	Solid	Vented	
Low squeal	6	8	
High squeal	114	79	
TUF	120	87	

prevalence of high squeal, while Duplex and Simplex systems demonstrate inferior performance in this aspect. Furthermore, the Heavy systems have a total number of unstable(TUF) of 90, suggesting considerably superior friction efficiency compared to the other configurations. However, not all of these modes result in squeal. Vibrational modes that are slightly unstable in theory may never become unstable in reality due to dissipative damping in an actual brake system [38]. These unstable modes, while not generating noise, can cause other issues in the structure such as gaps, structural damage, and increased wear on components, ultimately reducing their useful life.

This article presents the design of various brake systems (Figure 2) aimed at developing a finite element model that facilitates the analysis of the brake squeal phenomenon through complex eigenvalue analysis in the frequency domain. The modal analysis was performed to extract the complex eigenvalues for the vibrating modes of the disc brake system up to 25 kHz. When there are modes coupled at the same frequency, one of them becomes unstable. The unstable modes can be identified during complex eigenvalue analysis, because the real parts of the complex eigenvalues are positive (Figure 4). Those modes are prone to generate instabilities [22].

4. Results and Discussions

The instability prediction model for brake systems discussed in this paper employs a partially disturbed modal analysis. Figure 1 presents a flowchart outlining the adopted process to investigate the influence of input parameters on instability generation, also known as

sensitivity analysis. By varying the input parameters, we can observe their effects on the output parameters. This analysis facilitates the development of a parameter sensitivity profile. All operational and material parameters were taken from Table 3, varying only the friction coefficient for each brake system model, with a maximum friction coefficient of 0.4 and a minimum of 0.15.

To evaluate the performance of brake systems, three objectives were established, relating the effect of friction variation in solid and ventilated brake systems for cars, motorcycles, and trains, as well as in heavy, simplex, and duplex drum brakes (Figure 2). By analyzing these friction variations, the study aims to gain a deeper understanding of how different brake systems respond to changes in friction, particularly in terms of their tendency to produce brake squeal.

1. Maximize first unstable frequency FUF,  $\min \omega_i$  for  $\sigma_i$  positive;
2. Minimize TUF, the total number of unstable frequency,  $\sum_i$  for  $\sigma_i$  positive (in the given frequency range of analysis);
3. Minimize NI, noise index. In terms of the noise index (NI), an brake system may exhibit many unstable vibration modes within the audible frequency range. However, not all of these modes result in squeal. Vibrational modes that are slightly unstable in theory may never become unstable in practice due to dissipative damping in a real brake system. To compare the squeal propensity among unstable vibrational modes, the magnitude of the instability has traditionally been used as a noise index. In this study, the noise index was defined as Yuan [37, 38] for each vibration mode;

$$NI = \frac{\omega_i}{\sqrt{\omega_i^2 + \sigma_i^2}} \times 100\% \quad (i = 1, 2 \dots) \quad (19)$$

Where,  $\sigma_i$  is the instability of the system (real part) and  $\omega_i$  is the natural frequency of the system (imaginary part). The greater the noise index the more likely the corresponding mode was considered to cause audible squeal noise.

4.1. Solid and vented motorcycle disc brakes

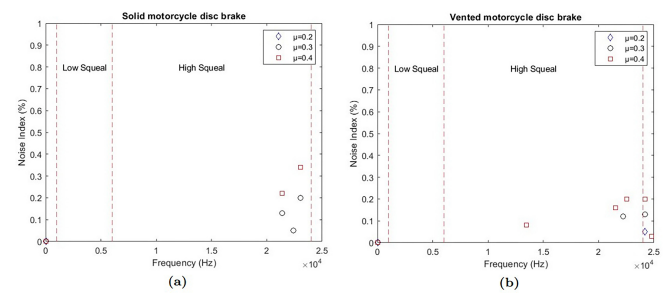
Table 4 and Figure 5 present the analysis of the influence of friction coefficient variation (0.15, 0.30, 0.45) on solid and vented motorcycle disc brakes in terms of squeal, total unstable frequencies (TUF), first unstable frequency (FUF), and noise index (NI).For solid motorcycle disc brakes, the results indicate that low squeal does not significantly occur except at a friction coefficient of 0.30, where a minor presence of squeal was detected. High squeal appears only at the highest coefficient (0.45), with a corresponding rise in TUF from 0 to 12 and 4. The FUF values suggest that instability begins around 21,376 Hz as friction increases. The noise index also rises notably

**Table 3:** Nominal brake systems parameters.

Parameter name	Notation	Value
Vented and Solid Car Disc Brakes		
Friction coefficient	$\mu$	0.30
Disc Speed	$\omega$	5 rad/s
Pressure	P	0.7 MPa
Disc Young's modulus	$E_{\text{Disc}}$	1.25 E +11 Pa
Back Plate Young's modulus	$E_{\text{Back Plate}}$	2.1 E +11 Pa
Pad Young's modulus	$E_{\text{Pad}}$	2.6 E +9 Pa
Disc density	$\gamma_{\text{Disc}}$	7155 kg/m <sup>3</sup>
Back Plate density	$\gamma_{\text{Back Plate}}$	7850 kg/m <sup>3</sup>
Pad Material density	$\gamma_{\text{Pad}}$	2045 kg/m <sup>3</sup>
Disc Poisson's ratio	$\nu_{\text{Disc}}$	0.23
Back Plate Poisson's ratio	$\nu_{\text{Back Plate}}$	0.3
Pad Material Poisson's ratio	$\nu_{\text{Pad}}$	0.34
Vented and Solid Motorcycle Disc Brakes		
Friction coefficient	$\mu$	0.30
Disc Speed	$\omega$	2.2 rad/s
Pressure	P	11.85 MPa
Disc Young's modulus	$E_{\text{Disc}}$	1.25 E +11 Pa
Back Plate Young's modulus	$E_{\text{Back Plate}}$	2.1 E +11 Pa
Pad Young's modulus	$E_{\text{Pad}}$	11.13 E +9 Pa
Disc density	$\gamma_{\text{Disc}}$	7155 kg/m <sup>3</sup>
Back Plate density	$\gamma_{\text{Back Plate}}$	7850 kg/m <sup>3</sup>
Pad Material density	$\gamma_{\text{Pad}}$	2045 kg/m <sup>3</sup>
Disc Poisson's ratio	$\nu_{\text{Disc}}$	0.23
Back Plate Poisson's ratio	$\nu_{\text{Back Plate}}$	0.3
Pad Material Poisson's ratio	$\nu_{\text{Pad}}$	0.34
Vented and Solid Railway Disc Brakes		
Friction coefficient	$\mu$	0.30
Disc Speed	$\omega$	0.5 rad/s
Pressure	P	0.5 MPa
Disc Young's modulus	$E_{\text{Disc}}$	1.20 E +11 Pa
Back Plate Young's modulus	$E_{\text{Back Plate}}$	2 E +11 Pa
Pad Young's modulus	$E_{\text{Pad}}$	7.57 E +9 Pa
Disc density	$\gamma_{\text{Disc}}$	7550 kg/m <sup>3</sup>
Back Plate density	$\gamma_{\text{Back Plate}}$	7850 kg/m <sup>3</sup>
Pad Material density	$\gamma_{\text{Pad}}$	2516 kg/m <sup>3</sup>
Disc Poisson's ratio	$\nu_{\text{Disc}}$	0.3
Back Plate Poisson's ratio	$\nu_{\text{Back Plate}}$	0.3
Pad Material Poisson's ratio	$\nu_{\text{Pad}}$	0.25
Heavy, Duplex and Simplex Drum Brakes		
Friction coefficient	$\mu$	0.30
Drum Speed	$\omega$	20 rad/s
Force	F	10000 N
Drum Young's modulus	$E_{\text{Drum}}$	1.25 E +11 Pa
Shoes Young's modulus	$E_{\text{Shoes}}$	1.7 E +10 Pa
Lining Young's modulus	$E_{\text{Lining}}$	1.1 E +11 Pa
Drum density	$\gamma_{\text{Drum}}$	7200 kg/m <sup>3</sup>
Shoes density	$\gamma_{\text{Shoes}}$	7200 kg/m <sup>3</sup>
Lining density	$\gamma_{\text{Lining}}$	2000 kg/m <sup>3</sup>
Drum Poisson's ratio	$\nu_{\text{Drum}}$	0.28
Shoes Poisson's ratio	$\nu_{\text{Shoes}}$	0.28
Lining Poisson's ratio	$\nu_{\text{Lining}}$	0.20

**Table 4:** Analysis of the variation in the coefficient of friction in solid and vented motorcycle disc brakes.

Solid motorcycle disc brake			
	0.15	0.30	0.45
Low squeal	0	2	0
High squeal	0	0	4
TUF	0	12	4
FUF	0 Hz	21376 Hz	21371 Hz
NI	0	0.2	2.4
Vented motorcycle disc brake			
	0.15	0.30	0.45
Low squeal	0	0	0
High squeal	2	3	6
TUF	2	3	6
FUF	24198 Hz	22211 Hz	13455 Hz
NI	0.05	0.2	0.3

**Figure 5:** Noise index for variations in the coefficient of friction; (a) Solid motorcycle disc brake; (b) Vented motorcycle disc brake.

from 0 to 2.4, signaling increased instability and noise at higher friction levels.

For vented motorcycle disc brakes, the trend is slightly different. High squeal is present at all friction levels, but the TUF remains relatively low. The first unstable frequency (FUF) decreases as friction rises, moving from 24,198 Hz to 13,455 Hz, implying that higher friction leads to more frequent low-frequency instability. The NI remains fairly low, suggesting a reduced noise risk compared to solid disc brakes, even as friction increases.

Overall, vented motorcycle brakes show better performance with lower NI values, indicating less noise potential compared to solid brakes, especially at higher friction levels. However, both systems demonstrate increasing instability with a higher coefficient of friction, especially in high squeal and total unstable frequencies (TUF).

## 4.2. Solid and vented car disc brakes

Table 5 and Figure 6 present the analysis of the influence of friction coefficient variation (0.15, 0.30, 0.45) on solid and vented car disc brakes in terms of



**Table 5:** Analysis of the variation in the coefficient of friction in solid and vented car disc brakes.

Solid car disc brake			
	0.15	0.30	0.45
Low squeal	0	0	0
High squeal	2	5	7
TUF	2	5	7
FUF	185154 Hz	5445.1 Hz	5466.2 Hz
NI	0.24	1.5	2.3

Vented car disc brake			
	0.15	0.30	0.45
Low squeal	0	0	0
High squeal	2	6	9
TUF	2	6	9
FUF	19081 Hz	15929 Hz	15451 Hz
NI	0.1	0.4	0.5

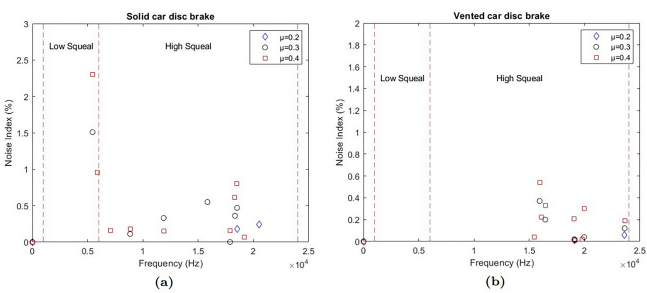


**Figure 6:** Noise index for variations in the coefficient of friction; (a) Solid car disc brake; (b) Vented car disc brake.

squeal, total unstable frequencies (TUF), first unstable frequency (FUF), and noise index (NI). For solid brakes, no low squeal was detected across all friction levels. High squeal occurrences increased significantly with friction, alongside a rise in TUF. Additionally, the FUF decreased substantially, while the NI showed a considerable increase, indicating higher noise susceptibility as friction increased. For vented brakes, the trend was similar regarding the absence of low squeal. However, high squeal and TUF were higher compared to solid brakes, though the FUF values also decreased. Despite these increases, the NI remained relatively low, suggesting vented brakes are slightly more stable in terms of noise generation compared to solid brakes.

The overall results indicate that vented brakes exhibit better performance at lower friction levels, particularly in terms of noise risk, but both brake types show increased instability and noise generation with rising friction.

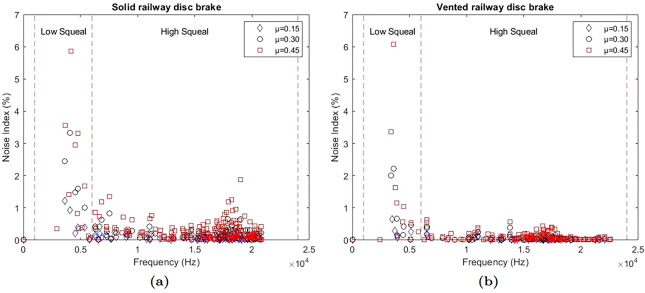
4.3. Solid and vented railway disc brakes

Table 6 and Figure 7 present the analysis of the influence of friction coefficient variation (0.15, 0.30, 0.45) on solid and vented railway disc brakes in terms of squeal, total

**Table 6:** Analysis of the variation in the coefficient of friction in solid and vented railway disc brakes.

Solid railway disc brake			
	0.15	0.30	0.45
Low squeal	6	6	12
High squeal	70	114	157
TUF	76	120	169
FUF	3627.4 Hz	3632.9 Hz	2916.9 Hz
NI	1.2	3.3	5.9

Vented railway disc brake			
	0.15	0.30	0.45
Low squeal	5	8	11
High squeal	39	79	132
TUF	44	87	143
FUF	3458.2 Hz	3362.9 Hz	3389.2 Hz
NI	0.6	2.2	6.1



**Figure 7:** Noise index for variations in the coefficient of friction; (a) Solid railway disc brake; (b) Vented railway disc brake.

unstable frequencies (TUF), first unstable frequency (FUF), and noise index (NI).

For the solid brake disc, as the friction coefficient increases, there is a rise in the TUF and in both low and high-frequency squeal. TUF ranges from 76 to 169, and high-frequency squeal increases significantly (from 70 to 157). The FUF decreases with the increase in friction, indicating that instabilities occur at lower frequencies as friction increases. For this brake disc model, the NI also grows significantly, from 1.2 to 5.9, indicating a higher propensity for noise with increased friction.

For the vented brake disc, the trend is similar, with TUF and high-frequency squeal increasing as the friction coefficient rises. However, the values are generally lower than for solid brakes. FUF decreases slightly with the increase in friction but remains within a close range (3458.2 Hz to 3389.2 Hz). NI rises sharply, ranging from 0.6 to 6.1, suggesting a greater susceptibility to noise at higher friction coefficients.

Vented brakes demonstrate better performance in terms of instability (lower TUF and NI) compared to solid brakes, especially at lower friction coefficients. This indicates that vented brakes may be more stable and less prone to noise generation, even with variations in friction coefficient. However, both systems show substantial

increases in instability risk as friction increases, with the NI in vented brakes being slightly more controlled than in solid brakes.

4.4. Heavy, duplex and simplex drum brakes

Table 7 and Figure 8 present the analysis of the influence of friction coefficient variation (0.15, 0.30, 0.45) on Heavy, Duplex and Simplex drum brakes in terms of squeal, total unstable frequencies (TUF), first unstable frequency (FUF), and noise index (NI).

For the heavy drum brake, the number of low squeals increases significantly from 4 to 14 as the coefficient of friction rises from 0.15 to 0.45, indicating a greater likelihood of low-frequency noise at higher friction levels. The occurrences of high squeal increase from 37 to 117 with the rise in friction, suggesting that higher friction is correlated with a greater incidence of high-frequency squeals, which may contribute to perceived noise and instability. The Total Unstable Frequencies (TUF) show a notable increase from 41 to 131, reinforcing the idea that increased friction leads to more unstable behavior in the braking system. The First Unstable Frequency (FUF) decreases significantly from 4144.8 Hz to 1415.4 Hz as friction increases, indicating that instabilities manifest at lower frequencies with higher friction levels. The Noise Index (NI) rises from 0.4 to 3.0, suggesting that higher levels of friction not only contribute to more occurrences of squeals but also to a greater potential for noise generation.

Table 7: Analysis of the variation in the coefficient of friction in Heavy, Duplex and Simplex drum brakes.

	Heavy drum brake		
	0.15	0.30	0.45
Low squeal	4	9	14
High squeal	37	81	117
TUF	41	90	131
FUF	4144.8 Hz	2249.9 Hz	1415.4 Hz
NI	0.4	2.0	3.0
	Duplex drum brake		
	0.15	0.30	0.45
Low squeal	0	0	0
High squeal	8	18	25
TUF	8	18	25
FUF	19256 Hz	6113.9 Hz	6099.4 Hz
NI	0.4	1.5	2.65
	Simplex drum brake		
	0.15	0.30	0.45
Low squeal	0	0	1
High squeal	14	25	35
TUF	14	25	36
FUF	6469.5 Hz	6459.6 Hz	3961.3 Hz
NI	0.6	1.2	2.2

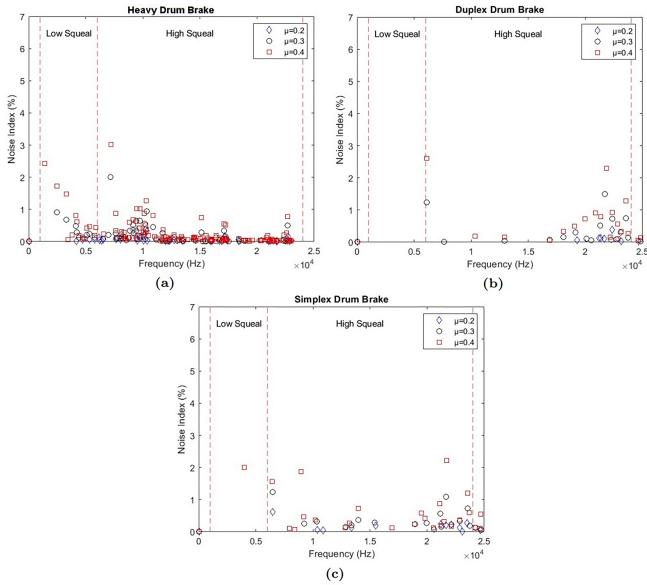


Figure 8: Noise index for variations in the coefficient of friction; (a) Heavy drum brake;(b) Duplex drum brake;(c) Simplex drum brake.

The Duplex Drum Brake does not exhibit occurrences of low squeals at any friction levels, indicating effective control over low-frequency instability. The occurrences of high squeals increase from 8 to 25, demonstrating that although duplex brakes are less prone to low squeals, they still experience an increase in high-frequency squeals with rising friction. Corresponding to the high squeal values, the TUF varies from 8 to 25, indicating a consistent relationship between the two parameters. The FUF starts at 19256 Hz and decreases to about 6099.4 Hz, suggesting that higher frictions cause instabilities to occur at lower frequencies. The NI increases from 0.4 to 2.65, indicating that duplex drum brakes, while generally stable, are still susceptible to increased noise as friction grows.

For the simplex drum brake, there is a minimal increase in occurrences of low squeals, rising from 0 to 1 as the coefficient of friction increases, reflecting stable performance in this regard. The occurrences of high squeals show a substantial increase from 14 to 35, indicating a greater likelihood of high-frequency noise with increased friction. The TUF values increase from 14 to 36, indicating a clear relationship between high squeal occurrences and overall instability. The FUF remains relatively stable, oscillating between 6469.5 Hz and 3961.3 Hz, suggesting a more consistent response in terms of instability frequency across all friction levels. The NI increases from 0.6 to 2.2, suggesting a moderate correlation between friction and noise potential, although this is lower than that observed in heavy drum brakes.

This analysis illustrates that an increase in the coefficient of friction generally leads to a higher number of occurrences of both low and high squeals in all types

of drum brakes analyzed. The heavy drum brake is the most affected, with significant increases in TUF and NI, indicating a higher risk of instability and noise. On the other hand, the duplex drum brake is more effective at mitigating low squeals, but still shows increases in high-frequency noise. The simplex drum brake shows moderate performance, with a notable increase in high squeals but minimal occurrences of low squeals.

## 5. Conclusion

Solid motorcycle disc brakes show minimal low squeal, occurring only at higher friction levels, while high squeal appears only at the highest coefficient, linked to an increase in TUF. Instability begins at higher friction, with a notable rise in the Noise Index (NI), indicating increased noise.

In contrast, vented motorcycle disc brakes exhibit high squeal at all friction levels, though TUF remains low. The FUF decreases with increased friction, suggesting more frequent low-frequency instability, while NI stays low, indicating reduced noise risk compared to solid brakes. In general, vented brakes demonstrate superior performance with lower NI values; however, both systems encounter heightened instability as friction increases, especially concerning high squeal and TUF.

For car solid brakes, no low-frequency squeal was detected at any friction level, while high-frequency squeal increased as friction rose. Instabilities occurred at lower frequencies with higher friction, and noise generation tendencies also grew. In car vented brakes, there was no low-frequency squeal across all friction levels. However, high-frequency squeal and instability were slightly more prominent compared to solid brakes. Despite this, vented brakes showed lower noise risks. Overall, while vented brakes offer better stability against low-frequency squeal, they are slightly more susceptible to high-frequency squeal and instabilities at higher friction levels than solid brakes.

The analysis of railway brake disc systems reveals that as the friction coefficient increases, solid brake discs experience a significant rise in TUF and occurrences of both low and high-frequency squeal. The FUF decreases, indicating that instabilities occur at lower frequencies with higher friction, while the Noise Index NI increases, suggesting a greater likelihood of noise generation.

In contrast, vented brake discs show improved stability, with lower TUF and NI compared to solid discs, especially at lower friction levels. Although vented brakes exhibit similar trends in increasing TUF and high-frequency squeal with rising friction, their values remain lower than those of solid brakes. The FUF for vented discs decreases slightly but stays within a narrow range, and the NI rises sharply, indicating increased noise susceptibility at higher friction coefficients. Overall, although both systems show greater instability and

increased noise risks as friction rises, vented brakes typically provide better performance and stability compared to solid brake discs.

The analysis of drum brake systems shows varying behaviors as friction levels increase. Heavy drum brakes experience a significant rise in both low and high-frequency squeals, alongside increases in TUF and NI. The simplex drum brake exhibits minimal low squeals, with moderate increases in high squeals and corresponding TUF values, indicating a link between high squeal occurrences and instability. The duplex drum brake effectively prevents low-frequency noise, recording no low squeals, but shows an increase in high squeals and a consistent rise in TUF, along with a decrease in the FUF. Overall, all drum brake types demonstrate a correlation between higher friction and increased noise occurrences, with differing susceptibility to instability and squealing.

The developed model has demonstrated a significant capability to simulate the phenomenon of noise in brake systems, providing a comprehensive analysis of the main characteristics involved. By focusing on the variables that affect noise generation, such as the coefficient of friction, the frequency of instabilities, and the noise index, the model offers valuable insights that can be applied in both education and research. For students, this tool can be especially useful as a teaching resource, allowing them to visualize and understand the complex dynamics occurring in brake systems. For researchers, the model serves as a robust platform for investigating new materials and designs for brake systems.

## References

- [1] A. Akay, *Acoustical Society of America* **111**, 1525 (2002).
- [2] J. Archard, *Journal of Applied Physics* **24**, 981 (1953).
- [3] A. Dias, R. Rodrigues, R. Bezerra and P. Lamary, *Noise & Vibration Worldwide* **53**, 49 (2022).
- [4] A.L. Dias, R.N. Rodrigues, R.A. Bezerra, P. Lamary and M.H.P. Miranda, *Proceedings of the Institution of Mechanical Engineers, Part C* **235**, 2797 (2021).
- [5] M.H.P. Miranda, R.N. Rodrigues, R.A. Bezerra, P.M.C. Lamary and R.A.O. Neto, *J. Braz. Soc. Mech. Sci. Eng.* **42**, 239 (2020).
- [6] M.H.C. Maciel, R.N. Rodrigues, C.A.S. Costa, R.A. Bezerra, V.V. Gonçalves and T.V.A. Freitas, *Proceedings of the Institution of Mechanical Engineers* **239**, 100 (2024).
- [7] R.T. Spurr, *Proceedings of the Institution of Mechanical Engineers: Automobile Division* **15**, 33 (1961).
- [8] N.M. Kinkaid, O.M. O'Reilly and P. Papadopoulos, *Journal of Sound and Vibration* **267**, 105 (2003).
- [9] J. Hultén, *SAE Technical Paper Series*, 951280 (1995).
- [10] L.T. Matozo, M.R.F. Soares and H.A. Al-Qureshi, *SAE Technical Paper*, 2008-01-2534 (2008).
- [11] K. Dunlap, M. Riehle and R. Longhouse, *SAE Technical Paper*, 1999-01-0142 (1999).
- [12] H. Ouyang, W. Nack, Y. Yuan and F. Chen, *International Journal of Vehicle Noise and Vibration* **1**, 207 (2005).

- [13] P. Grange, D. Clair, L. Baillet and M. Fogli, *Mechanical Systems and Signal Processing* **23**, 2575 (2009).
- [14] A. Elmaian, F. Gautier, C. Pezerat and J.M. Duffal, *Applied Acoustics* **76**, 391 (2014).
- [15] N.M. Ghazaly, M. El-Sharkawy and I. Ahmed, *J. Mech. Des. Vib.* **1**, 5 (2014).
- [16] S. Ganguly, H. Tong and Y. Karpenko, *SAE Technical Paper Series*, 2008-01-2531 (2008).
- [17] A.L. Dias, R.N. Rodrigues, R.A. Bezerra and P. Lamary, *J. Vib. Eng. Technol.* **9**, 2019 (2021).
- [18] A. Dias, R. Rodrigues, R. Bezerra, P. Lamary and M. Miranda, *Proceedings of the Institution of Mechanical Engineers, Part C: Journal of Mechanical Engineering Science* **235**, 6052 (2021).
- [19] J. Kang, *Journal of Sound and Vibration* **331**, 2190 (2012).
- [20] J. Huang, C.M. Krousgrill and A.K. Bajaj, *Journal of Sound and Vibration* **289**, 245 (2006).
- [21] M.T. Júnior, S.N.Y. Gerges and R. Jordan, *Applied Acoustics* **69**, 147 (2008).
- [22] M. Nouby and K. Srinivasan, *Jurnal Mekanikal* **69**, 147 (2009).
- [23] G. Liles, *SAE Technical Paper Series*, 891150 (1989).
- [24] P. Forte, F. Frendo and R.N. Rodrigues, *Journal of Physics: Conference Series* **5744**, 012239 (2016).
- [25] T.V.A. Freitas, R.N. Rodrigues, C.C.A. Santos, R.A. Bezerra, V.V. Gonçalves and M.H.C. Maciel, *Proceedings of the Institution of Mechanical Engineers, Part J: Journal of Engineering Tribology* **238**, 1433 (2024).
- [26] R.N. Rodrigues, G. Achtenová, L. Kazda, V. Klír, V.V. Gonçalves, R.A. Bezerra and M.H.C. Maciel, *Noise & Vibration Worldwide* **55**, 438 (2024).
- [27] M.H.C. Maciel, R.N. Rodrigues, C.A.S. Costa, R.D.A. Bezerra, V.V. Gonçalves and T.V.A. Freitas, *Noise & Vibration Worldwide* **54**, 570 (2023).
- [28] Y.K. Wu, B. Tang, Z.Y. Xiang, H.H. Qian, J.L. Mo and Z.R. Zhou, *Applied Acoustics* **171**, 107540 (2021).
- [29] Q. Zhu, J. Xie, W. Zhang, G. Chen and J. Tuo, *Wear* **522**, 204884 (1989).
- [30] S. Ahn, C. Sohn, S. Choi and C. Nam, *Journal of Mechanical Science and Technology* **37**, 2253 (2023).
- [31] S. Ahn, C. Nam, S. Choi, D. An, I. Kim, K. Seo and C. Sohn, *Journal of Mechanical Science and Technology* **35**, 1923 (2021).
- [32] F. Cascetta, F. Caputo and A. Luca, *Advances in Acoustics and Vibration* **2018**, 4692570 (2018).
- [33] Z. Sha, J. Lu, Q. Hao, J. Yin, Y. Liu and S. Zhang, *Appl. Sci.* **12**, 10739 (2022).
- [34] A. Belhocine and N.M. Ghazaly, *Latin American Journal of Solids and Structures* **12**, 1432 (2015).
- [35] A. Belhocine, *Int J Adv Manuf Technol* **12**, 3563 (2017).
- [36] A. Belhocine and W.Z.W. Omar, *J. Mech. Sci. Technol.* **12**, 481 (2018).
- [37] Y. Yuan, *Proceedings of the ASME* **34**, 17 (1995).
- [38] I. Ahmed and S. Aboul-Seoud, *SAE Technical Paper*, 2006-01-3211 (2006).